arXiv:1202.3327v1 [cond-mat.supr-con] 15 Feb 2012

Electric Field induced Superconductivity in Multigraphene

A. Ballestar,[1] J. Barzola-Quiquia,[1] S. Dusari,[1] P. Esquinazi,[1, *] R. R. da Silva,[2] and Y. Kopelevich[2]
[1] *Division of Superconductivity and Magnetism, Institut für Experimentelle Physik II,*
Universität Leipzig, Linnéstraße 5, D-04103 Leipzig, Germany
[2] *Instituto de Física "Gleb Wataghin"/DFA, Rua Sergio Buarque de Holanda Nr.777,*
Universidade Estadual de Campinas-UNICAMP, Cidade Universitária Zeferino Vaz, Bairro Barão Geraldo 13083-859, Brasil

We have studied the temperature and magnetic field dependence of the electrical resistance of mesoscopic, tens of nanometers thick multigraphene samples as a function of a bias voltage applied perpendicular to the graphene planes. We found that the resistance changes asymmetrically with the bias voltage sign. For large and negative bias voltages the resistance shows a non-percolative superconducting-like transition at $T \sim 15 \ldots 20$ K. A large enough magnetic field suppresses the transition.

I. INTRODUCTION

Recently published studies show that electrostatic carrier accumulation is an interesting tool to trigger new states of matter at certain interfaces. Electric field induced quasi-two dimensional (2D) superconductivity has been reported in the insulating oxide $SrTiO_3$,[1] on an atomically flat ZrNCl film[2], on $KTaO_3$ single crystals[3], in $LaTiO_3/SrTiO_3$ hetero-structures[4], with critical temperatures ranging from 0.05 K to 15 K, after inducing 2D carrier densities between $\sim 10^{13}$ cm^{-2} and $\sim 10^{14}$ cm^{-2}, upon material or interface studied. The idea to trigger 2D superconductivity by inducing excess charge at the surface of a dielectric sample by the application of an electric field was proposed already in Ref. 5 for the particular case of the surface region of La_2CuO_4 assuming a weak coupling between the CuO_2 layers.

The possible existence of superconductivity in graphite and in graphene has been a subject of experimental[6] as well as theoretical interest in the last 10 years. For example, p-type high-T_c superconductivity has been predicted to occur in inhomogeneous regions of the graphite structure[7] or $d-$wave superconductivity based on resonance valence bonds[8]. Following a BCS approach in two dimensions energy gap values at 0 K of the order of 60 K have been obtained if the density of conduction electrons per graphene plane increases to $n \sim 10^{14}$ cm^{-2},[9] in agreement with the theoretical predictions based on different others approaches.[10,11] Also room temperature superconductivity with a $d + id$ pairing symmetry has been predicted to occur in doped graphene with a carrier concentration $n \gtrsim 10^{14}$ cm^{-2}.[12]

We expect that if one can trigger superconductivity in quasi-2D regions of graphite as well as at doped surfaces[13] it may exist at much higher temperatures than in the basically 3D superconducting intercalated graphitic compounds.[14] This expected difference in critical temperatures and within a mean field model can be partially understood taking into account the role of high-energy phonons in the 2D graphite structure itself.[9] Since most of the theoretical predictions emphasize that superconductivity should be possible under the premise that the carrier density per graphene area is high enough to reach $T_c > 1$ K,[9–11] it is then appealing to use the electrostatic charge doping to increase n in graphite without disturbing its quasi-2D dimensionality. We note that the intrinsic carrier density of defect-free graphene layers inside graphite is $n < 10^9$ cm^{-2}.[15,16] However, defects and/or hydrogen doping within regions at interfaces[17] or at the graphite surface may show much larger carrier density, e.g. $n \sim 10^{11}$ cm^{-2}, as literature values indicate. Therefore, if we can increase the carrier density above some critical value we may expect to trigger superconductivity in those regions with carrier densities just below a certain value. We note further that the surface region of graphite appears then to be especially interesting according to recently published theoretical work[18] that emphasizes that this may show a topologically protected flat band promoting superconductivity at very high temperatures.

II. EXPERIMENTAL DETAILS AND SAMPLES CHARACTERISTICS

We have studied five multigraphene (thin graphite flakes) samples named S1 . . . S5. Samples S1 and S3 were graphite flakes of $\simeq 40$ μm length, see Fig. 1, and with a non homogeneous thickness ranging between 20 nm and 40 nm. Samples S2 and S5 showed a homogeneous thickness of 40 nm and $\simeq 15$ μm length. Sample S4 of 90 nm thickness was the thickest of all studied samples in this work. All samples were prepared by a rubbing method and fixed on the 150 nm thick SiN part of a doped Si substrate following a similar procedure as shown in Ref. 17.

The contacts of the sample were prepared by electron lithography using Pd/Au thermal evaporated electrodes, see Fig. 1 (up right). The bias voltage was applied through a fifth electrode. The results shown in this work did not depend whether we apply the bias voltage at the electrode at the edge, as shown in Fig. 1 (bottom), or at some of the other electrodes.

The resistance was measured with AC and DC input currents. In case of application of a bias voltage we used a DC current of 1 μA with a Keithley 6221 current source and the voltage measurements were done with a Keithley 2182 DC nanovoltmeter. The AC measurements were performed using a LR700 AC resistance bridge from Lin-

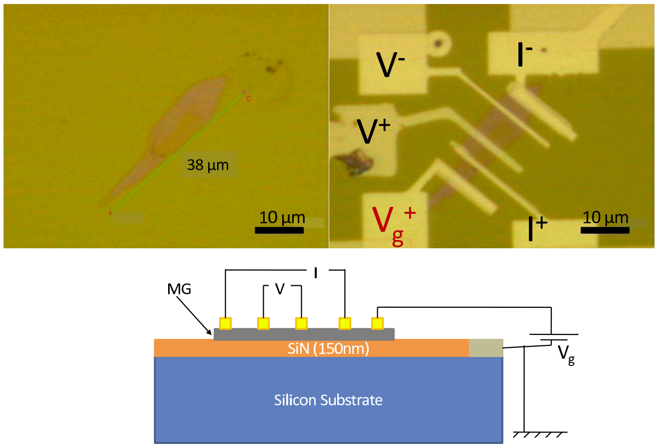

FIG. 1. The upper-left picture shows an optical image of the sample S1 just after the rubbing process on the SiN substrate. On the upper-right picture, the same sample after the lithography and Pt-Au thermal evaporation. The voltage, current and bias voltage electrodes are indicated as they have been used in the whole set of measurements. In the bottom picture, a sketch of the configuration used in this work is shown. MG represents the multigraphene sample, and the labels V and I the voltage and current electrodes. For positive bias voltages $V_g > 0$, the positive electrode is connected to one of the contacts on the sample surface as shown in the sketch.

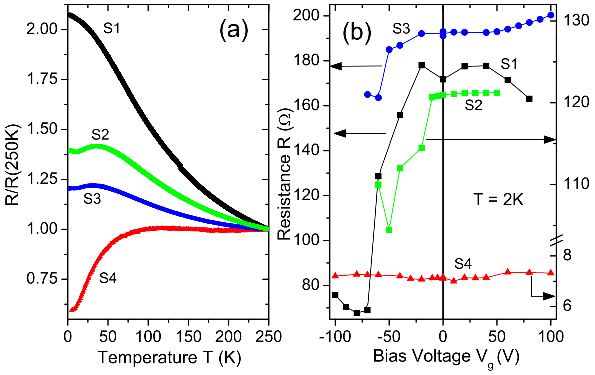

FIG. 2. (a) Temperature dependence of the normalized resistance of four samples at zero bias voltage and zero applied magnetic field. The amplitude of the input AC current was 1μA. (b) Bias voltage dependence of the resistance for samples S1 and S3 (left $y-$axis), S2 and S4 (right $y-$axis) at 2K and no applied magnetic field.

ear Research.

The temperature dependence of the resistance $R(T)$ at zero bias voltage has been measured for every sample and it is shown in Fig. 2(a). S1, S2 and S3 samples show a semiconducting behavior intrinsic to the graphite Bernal structure according to the work done in Ref. 19. The level off of $R(T)$ of sample S1 below 25 K or the features below 50 K in samples S2 and S3 and the metallic like behavior of S4 are due to the contributions of the surface of the sample (or sample-substrate) and/or due to the internal interfaces in the sample, as discussed in Refs. 17 and 19. As expected, the thicker S4 sample shows a metallic behavior below 100 K, which is related to the higher number of internal interfaces as reported in detail in Ref. 17. These internal interfaces have a much larger carrier density as the graphene layers within the defect free regions of graphite. Therefore, we expect that in thicker samples the shielding of the electric field is much larger than in thinner ones, as we describe below.

III. BIAS VOLTAGE DEPENDENCE OF THE RESISTANCE

A. Electrostatic screening in multigraphene samples

The electrostatic screening in multigraphene samples is essential since without a large amplitude of the electric field in the sample through the applied bias voltage we will see no effect on the electrical resistance. To estimate the penetration depth of the applied electric field inside our samples we use a recently published theoretical paper[20], which emphasizes that the actual screening depth depends on the experimental conditions, in particular the actual doping of the sample. The intrinsic carrier density in each graphene layer in the graphite structure without defects and interfaces should be $n < 10^9$ cm^{-2} at the temperature of our experiments.[15,16,21] The exact value of n for the graphene layers in each of the measured samples is not really well known just because the samples are not free from defects and impurities as, e.g., hydrogen. Due to the relatively low temperatures of our measurements we take as upper limit $n \sim 10^8$ cm^{-2} for the graphene layers not involved in the internal interfaces or at the surface. In case the carrier density n of the non-defective graphene layers is smaller, then the larger will be the penetration depth of the electric field in the sample. Although Ref. 20 assumed a zero energy gap for Bernal graphite, the magnitude of the used voltages in our experiments is much larger than the experimentally obtained semiconducting gap of ~ 40 meV.[19] Therefore and following Ref. 20 we estimate that at $T < 30$ K the effective penetration depth should be equal to at least 7 graphene layers or about 2.4 nm. That would mean that the electric field mainly influences the near surface region of the samples, in case that no internal interfaces with much larger carrier density exist. Otherwise, as we will see for sample S4, these interfaces appear to largely screen the applied field and no effect is observed after application of a bias voltage.

Our estimate is basically in agreement with other theoretical work, which showed that the electric field should be screened within a few layers from the sample surfaces.[22] Therefore, an estimation for the electric field penetration depth of at least 3 to 10 graphene layers from the surface appears realistic. Note that due to the large electrical resistance of the SiN layer and taking into account its capacitance ($\sim$ 10 nF), of the same order as the effective capacitance of the multigraphene samples, we expect large equilibrium relaxation times in the range of $\tau = RC \gtrsim 5 \times 10^3$ s (R, C are the total resistance and capacitance parallel to the applied electric field).

Finally, we note that the bias voltage is applied between the top of the Si substrate and the top surface of the samples. This means that we have a distance between electrodes of 150 nm plus the thickness of the samples, i.e. between 170 nm to 240 nm. This effective thickness difference of $\lesssim$ 40% between the samples, and within a rough linear capacitor model, would indicate a reduction of the same order in the electric field amplitude for the same bias voltage between the thinnest and thickest samples. We will see below, however, that it is not only the thickness the parameter that determines the amplitude of the effect of the electric field but the highly conducting interfaces, which have a mean distance between 30 nm and 100 nm inside the graphite structure of the studied samples.[17]

B. Bias voltage dependence at constant temperature

Figure 2(b) shows the resistance vs. applied bias voltage V_g at a constant temperature of 2 K without applying any magnetic field. Starting from zero bias voltage we increased to positive V_g values, then we returned to zero and measured the resistance for the negative range of V_g. Each point in Figure 2(b) was measured after reaching equilibrium at each point till the resistance did no change with time. The curves shown in Fig. 2(b) are reversible, demonstrating the electrostatic nature of the observed effects.

The samples S1, S2 and S3 show an asymmetric behavior respect to zero voltage. For positive voltage, i.e. the electric field direction points towards the sample and substrate, the resistance does not change significantly. In the case of sample S1 it slightly decreases after +50V. The resistance of S2 does not change up to +60V, and finally the S3 resistance increases slightly for $V_g > +50$ V.

For negative V_g, however, a remarkable decrease of the resistance appears. A minimum value in the measured resistance is reached for slightly different negative bias voltages upon sample. For sample S2 the minimum of resistance appears at -50V, for S3 at -60V and for S1, which shows the largest change, at ~ -75 V. As will become clear in the discussions below, these differences, as well as that in the relative decrease of resistance at a given bias voltage, are related to the carrier inhomogeneity of the multigraphene samples. Note that for the thickest sample S4 the resistance does not show any significative change with V_g. This is a clear indication for the screening effect of the electric field by the internal interfaces mentioned previously. Would the electric field amplitude decreases simply proportional to the sample thickness, we expect to see a decrease in the resistance within the scanned V_g range. A similar behavior of the resistance of the multigraphene samples S1 to S4 with the applied bias voltage was partially reported in Ref. 23. However, in that work no results on the temperature or the magnetic field dependence of the resistance under a bias voltage were reported.

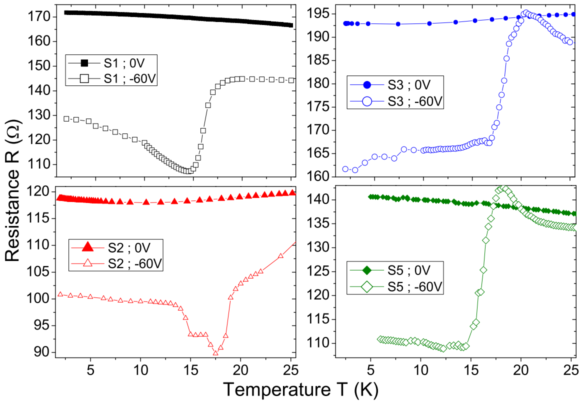

FIG. 3. Temperature dependence of the resistance for four of the multigraphene samples at $V_g = -60$ V and at no applied magnetic field.

C. Temperature dependence of the resistance under a bias voltage

The results of the resistance vs. bias voltage shown in Fig. 2 were obtained at a constant temperature of 2K. Taken into account these results, the aim of the next experiment was to investigate the change of the resistance with temperature at constant applied bias voltage. Figure 3 shows the temperature dependence of the resistance of four samples without and under $V_g = -60$ V. As one can easily realize and as it was shown before in Fig. 2(b), the resistance is in general smaller under -60 V. But remarkable is the fact that in all the samples a clear step like transition below 20 K appears. The details of the transition depends on the selected sample, again a sign of the existence of inhomogeneities in the samples.

Furthermore, the effect of the gate voltage values on the temperature dependence of the resistance was investigated in detail. Figures 4 and 5 show the results measured for samples S1 and S2, respectively. In the case of sample S1, the temperature behavior of the value as well as the temperature dependence of the resistance $R(T)$ does not change significantly for $-40V > V_g > +60V$. At $V_g = -40$ V a small dip in $R(T)$ appears at $T \simeq 17$ K.

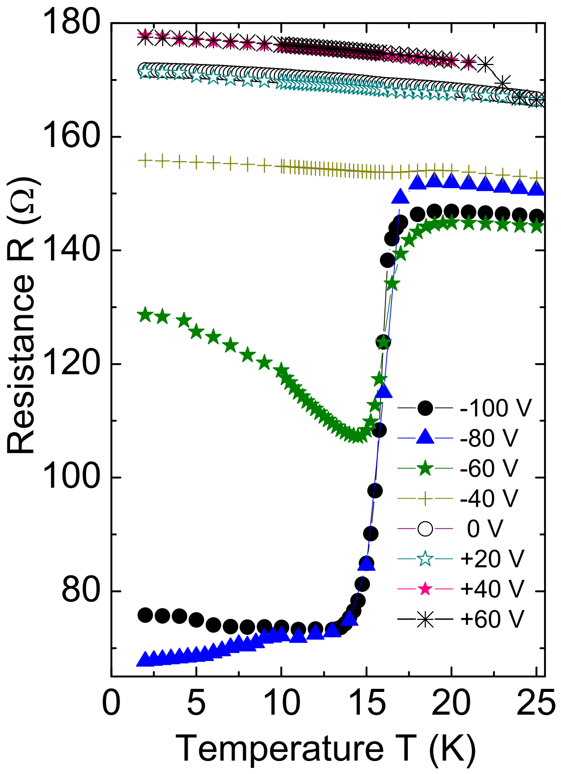

FIG. 4. Temperature dependence of the resistance of sample S1 at different constant values of V_g and no applied magnetic field.

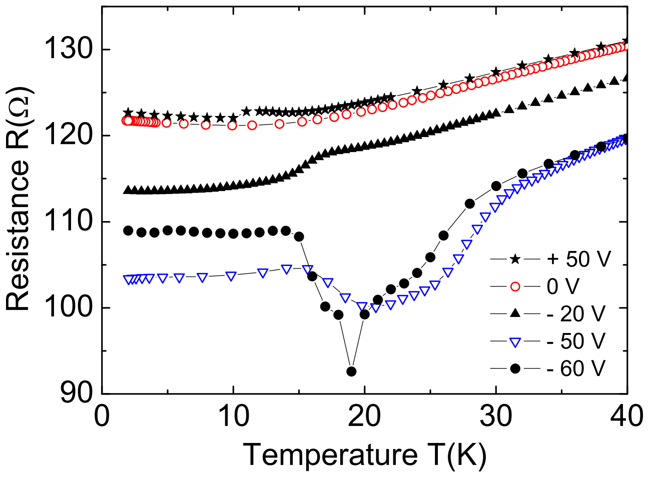

FIG. 5. Temperature dependence of the resistance of sample S2 at different constant values of V_g and no applied magnetic field.

For $V_g < -40V$ the small dip develops in a clear step at similar temperatures with less than 2 K transition width. The overall shape of these curves suggests the existence of a non-percolative superconducting transition, as the measured behavior with magnetic field also indicates. The curve obtained at $V_g = -60$ V with a drop at 15 K and an upturn below it are clear indications of a non-uniform channel with superconducting regions connected in series with normal ones in which partial charge localization effects occur. The clear asymmetric behavior of the resistance with V_g is recognized also in Fig. 4.

The lower the bias voltage the clearer the transition triggered by the change in the carrier density. Note that the apparent transition temperature does not shift significantly with the applied bias voltage. The overall behavior of the resistance $R(T)$ with applied V_g strongly resembles in several details the one obtained for ZrNCl flat thin film in Ref. 2, even in the obtained transition temperature. However, with one important difference, namely that in the multigraphene samples no superconducting percolating path is reached. We ascribe this behavior to the carrier inhomogeneities of the samples[24], a fact related to the large sensitivity of the carrier density of the graphite structure to defects and impurities.[15]

A similar, but not identical, behavior is obtained for sample S2, see Fig. 5. This sample shows already at -20 V applied bias voltage a clear step in the resistance starting at $\simeq$ 17 K. At higher negative voltages, however, the resistance starts to show signs of a transition at higher temperatures. It is clear that the details of the effects observed by the applied electric field depend on the multigraphene sample, again an evidence for the role that inhomogeneities play in the observed phenomenon.

D. Temperature dependence of the resistance under a magnetic field and bias voltage

To characterize the magnetic field behavior of the observed transition as a function of temperature we fixed the bias voltage to a large enough value taking into account the results shown in the last sections. In what follows we discuss mainly the results of sample S1 for both, magnetic field applied normal and parallel to the graphene planes. Results for the other samples are qualitatively similar. Figure 6 shows the dependence of the resistance (absolute (a) and relative (b)) with temperature at different applied fields normal to the main area of the sample and at a fixed bias voltage of -100 V. The measurements were performed as follows. At 2K a bias voltage of -100 V was applied. After reaching equilibrium the corresponding magnetic field was applied as well and the resistance was measured to 25 K. At 25 K the magnetic field was removed, the sample was cooled again to 2 K again and we repeated the same procedure for others magnetic field values. The bias voltage has been applied all the time.

As expected for this field direction, the background re-

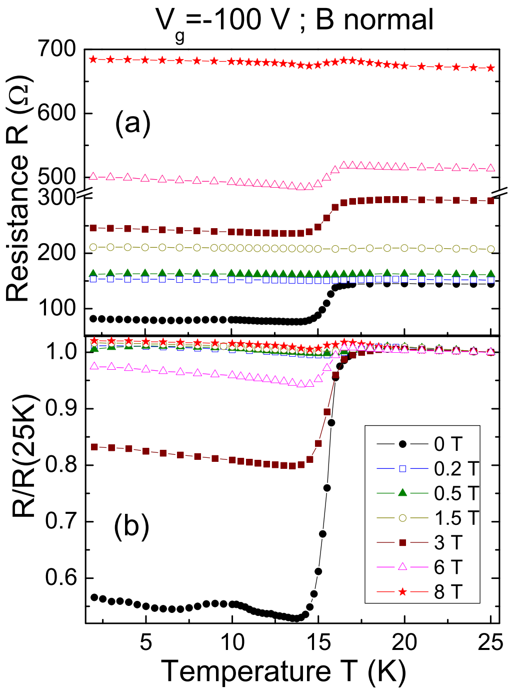

FIG. 6. Temperature dependence of the resistance of sample S1 at different constant values of magnetic field applied normal to the graphene planes and at $V_g = -100$ V. (a) Absolute values of the resistance. (b) Normalized values of the resistance by the resistance at 25 K vs. temperature at the same applied fields as in (a).

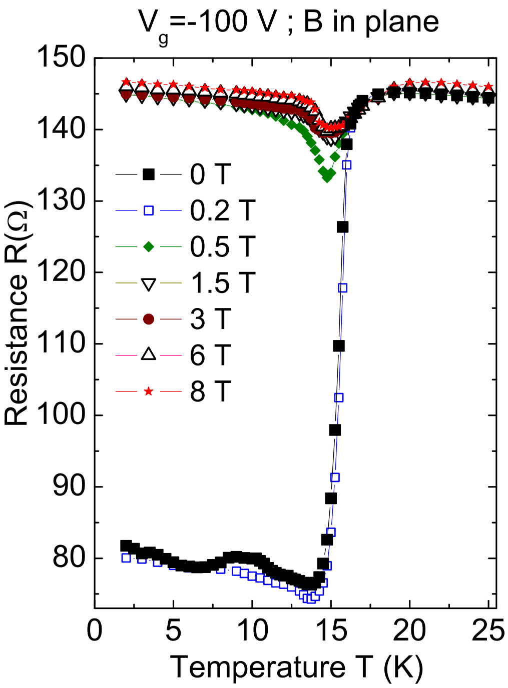

FIG. 7. Temperature dependence of the resistance of sample S1 at different constant values of the field applied parallel to the graphene planes and at $V_g = -100$ V.

sistance increases with field due to the usual magnetoresistance of the multigraphene samples, see Fig. 6(a). As shown in Fig. 6 a field of 0.2 T is enough to suppress completely the transition at 15 K. This suppression remains to a field of 1.5 T. At a field of 3 T and higher the transition appears again at the same temperature but slightly broader and nearly vanishing at 8 T, see Fig. 6(b). This non monotonous field behavior is observed for fields normal to the graphene planes only. Note that the temperature of the transition does not change significantly with applied field. The transition is rather unconventional because the magnetic field affects mainly the relative step height of the transition, see Fig. 6(b).

Figure 7 shows the resistance vs. temperature at $V_g = -100$ V and at different magnetic fields applied parallel to the graphene planes of the sample. The misalignment of the field is less than 0.5°. The measured data show that the transition remains unaffected by a parallel field of 0.2 T, in contrast to the normal field result. At higher fields, however, it is suppressed monotonously without any sign for a reentrance like in the other field direction. In Fig. 8 we compare the results for both field direction by plotting the minimum resistance just below the transition normalized by the resistance value at 25 K vs. applied field. As for the normal applied fields, for

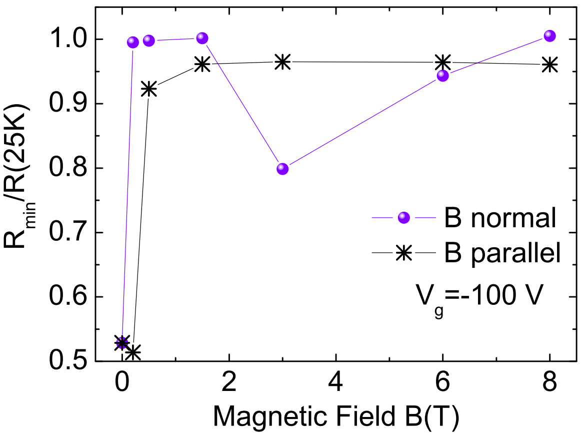

FIG. 8. Change of the resistance minimum normalized by the resistance value at 25 K for sample S1 with the magnetic field applied normal (•) and parallel ($*$) to the graphene planes of the sample and at $V_g = -100$ V.

parallel applied fields the transition does not shift significantly to lower temperatures and the resistance shows a minimum just below the transition. Note that the resistance above $\simeq 17$ K does not change practically with field in agreement with the fact that the magnetoresistance of graphite depends mainly on the normal field component to the graphene planes.[25]

IV. DISCUSSION

In this section we discuss the rather unconventional behavior of the electrical resistance under a bias voltage and its possible origin. We divide the discussion in three parts. In the first part (A) we show experimental evidence that supports an increase in the carrier density after application of a bias voltage in our multigraphene samples. In part (B) we discuss to what extent the observed transition can be considered as due to superconductivity or other kind of electronic transition. We emphasize the resemblance of the observed behavior with that obtained in the past for granular superconducting thin metallic films. We shortly review the main results of recently published work on graphite samples that suggest the existence of granular superconductivity in this material. In part (C) of this section we speculate on possible explanations for the anomalous magnetic field behavior of the transition, assuming that it is indeed related to superconductivity.

A. Increase of carrier density with bias voltage

The transition observed at $T \lesssim 20$ K in different multigraphene samples after the application of a negative bias voltage indicates that this happens after increasing enough the carrier density and the Fermi level. Taking into account the expected field penetration depth, we expect that the superconducting path is located at the upper near surface region of the samples. A way to check whether there is a real increase in the carrier density with applied bias voltage is to measure the Shubnikov-de Haas (SdH) oscillations of the magnetoresistance. Figure 9(a) shows the magnetoresistance of sample S1 at 2 K without and with an applied voltage. From these data we plot in Fig. 9(b) the first field derivative of the magnetoresistance vs. inverse field. At no applied bias voltage the data reveal no SdH oscillations in the shown field range and within experimental error, in agreement with the rather small carrier density of the graphene planes $n < 10^9$ cm^{-2}.[15,16,21]

At an applied bias voltage of -100 V clear SdH oscillations are observed in the first field derivative for fields above ~ 4 T. From the obtained period of the oscillations (lowest frequency $f \simeq 46$ T) we estimate a 2D carrier density $n \simeq 2.2 \times 10^{12}$ cm^{-2}, an order of magnitude larger that the one obtained for the bulk graphite sample (continuous line in Fig. 9(b)) from which the multigraphene samples were prepared. We stress that the carrier density obtained for the bulk sample is not intrinsic of the Bernal graphite structure but it originates mainly at the internal interfaces (or other defective regions, see Ref. 15) commonly found in the used highly oriented pyrolytic graphite samples.[17] As shown recently[15] the SdH oscillations in multigraphene samples depend on the sample position indicating the existence of inhomogeneities in the carrier concentration within micrometers. This picture agrees with the results obtained from electric field microscopy (EFM) that revealed submicrometer domain-like carrier density distributions in graphite surfaces.[24] On going experiments using an array of electrodes distributed on the same sample provide further evidence for the inhomogeneous response of the multigraphene samples after application of the bias voltage. This result also indicates the existence of inhomogeneities in the carrier distribution within the sample.

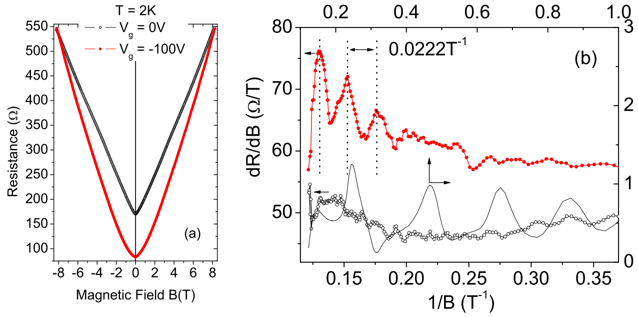

FIG. 9. (a) Magnetoresistance of sample S1 for normal to the graphene planes field, at 2 K and without and with an applied bias voltage. (b) First derivative of the magnetoresistance vs. inverse field from the data of (a) and for a bulk graphite sample of size $2 \times 1 \times 0.2$ mm^3 at 4 K (upper-right axes).

B. Can the observed transition be related to superconductivity?

The obvious question that needs an answer is the origin of the observed transition in the resistance when the carrier density increases. Leaving apart superconductivity, it appears difficult to find the origin in a kind of electron delocalization decreasing temperature. Also the fact that the magnetic field removes the transition appears to be at odd with electron localization effects. Note that a parallel magnetic field does not change the resistance above the transition, see Fig. 7, indicating clearly the absence of any Lorenz-force driven effect or a change in the electron system at all above the critical temperature.

One may speculate that the observed transition might be related to an electric field induced sliding motion of a charge-density wave (CDW), which may lower the resistance, and the existence of a strong coupling between a magnetic field and the CDW structure, as has been observed in NbSe_3, for example[26,27]. However, in the case we present here two observations appear to be at odd with a CDW origin. Namely, the transition at $T \sim 15$ K is sharp and within less than 3 K in contrast to the very broad decrease of the resistance due to the move of a CDW decreasing temperature under an applied electric field[26]. Second, we did not find any signature of nonlinearity of the resistance with current I below 10 μA at any applied magnetic or electric field (currents above this value can destroy the sample and were not applied), in contrast to the observations in CDW transitions[27,28]. Note that in case of a CDW the resistance becomes nonlinear at progressively lower currents as the magnetic field is increased[27].

The absence of nonlinearity at low currents may appear to be also at odd with the existence of granular superconductivity. However, the appearance of nonlinearities in the resistance in this case depends actually on the sample granular characteristics and current range. For comparison we refer to the extended work done on the onset of superconductivity in ultrathin granular metal films, see for example Refs. 29 and 30. The similarity of our results of the resistance vs. temperature for constant applied electric fields (see Figs. 3 and 4) with those found in non-percolative granular superconducting films[29] is appealing. We note that in the case of ultrathin superconducting Ga films the $I - V$ characteristics are rather linear at low enough currents and in films where no global superconductivity occurs[29].

On the other hand the existence of granular high-temperature superconductivity in regions within internal interfaces found in highly oriented pyrolytic graphite, has been proposed recently[17] as a possible answer to a series of experimental hints on its existence in oriented graphite samples published the last years. In short, the main experimental observations that suggest the existence of non-percolative superconducting regions in oriented graphite samples are: (1) Magnetic field driven metal-insulator transition (MIT)[31,32]. We should note that the MIT in graphite has been also interpreted in terms of the two band model using several magnetic field and temperature dependent free parameters[33]. However, this "transition" does not exist when the oriented graphite sample gets thinner than ~ 70 nm and therefore its origin is not intrinsic of the graphite ideal structure[17]; (2) Superconducting-like hysteresis loops in the magnetization of pure HOPG samples[6,34]; (3) Anomalous hysteresis in the low-field magnetoresistance of mesoscopic graphite samples, similar to those found in granular superconductors[35,36]; (4) Superconducting-like magnetic field driven transition in the resistance when measured near or at an internal interface of a graphite flake[37]; (5) Anomalous temperature dependence of the zero field resistance of oriented graphite samples, which follows an exponential, thermally activated behavior[19,38] similar to the one found in granular superconductors as in granular Al-Ge[39], for example. (6) Finally, Josephson-like $I - V$ characteristic curves found in especially prepared thin graphite transmission electron microscope (TEM) lamellas[40]. Apart from the hints in pure oriented graphite samples, experimental evidence for high-temperature superconductivity has been also reported in composite graphite - sulphur powders.[41–44] All this evidence indicates clearly an intrinsic tendency of the phenomenon of superconductivity to appear in certain regions of graphite after doping.

In order to reach a state of zero resistance in some part of the graphite sample, it is clear that one needs to have a doped region large enough that one or several Josephson coupled superconducting patches exist between the voltage electrodes. This appears still difficult to reach applying only an electric field in the samples used in this work. On the other hand results on thin TEM lamellae prepared with a large number of internal interfaces,[40] which show a carrier density similar or higher than the one we obtained in our samples after applying an electric field, shows a current dependent zero resistance state below 20 K. Taking into account this evidence and from the comparison with literature it appears natural to interpret the observed transition with electric field in our multigraphene samples as a sign of granular superconductivity.

C. Anomalous magnetic field behavior of the transition

The magnetic field behavior of the transition for both field directions, i.e. the resistance below the transition increases with field without a clear decrease of the transition temperature within the used field range, suggests that a filamentary superconducting path produced by the applied bias voltage, is affected by the magnetic field. Future experiments should clarify whether the superconducting channel connects localized superconducting "grains" or patches with much higher critical temperatures and fields.

The differences in the behavior observed as a function of field direction are also peculiar. From one side orbital effects appear to be important taking into account the suppression of the transition for a field of 0.2 T (for sample S1, for example) applied normal to the graphene planes only. Also the reentrance of the transition observed only for fields normal to the graphene planes appears to have an orbital character. We note that a similar effect has been observed through the measurement of the conductance of a high-mobility 2D electron gas between superconducting contacts at high fields applied normal to the main 2D area.[45] This reentrance or increase in the conductance with magnetic field was explained arguing the increase in the probability of Andreev reflections above a certain field.[45] A comparison of our results with those from Ref. 45 is permissible because the carriers mobility in the graphene layers of our samples is huge[16] and also hints for the influence of Andreev reflections in the magnetoresistance have been recently reported.[35]

On the other hand we should take into account that the transition is also affected by a parallel field. The absolute difference at low fields (for sample S1) between the two field directions cannot be explained by the small misalignment in the applied field direction and indicates that other mechanisms than orbital may play a role in the triggered superconducting state. The difference in the resistance behavior as a function of the field direction might be understood assuming the interaction between preexisting ferromagnetic moment and spin-polarized superconducting currents (SC) as was conjectured for superconducting graphite doped with sulfur.[46] The spin-polarized SC currents, associated with either p-wave spin-triplet[7] or d-wave superconducting order parameter[8] with breaking time-reversal symmetry, exert a torque on the ferromagnetic moments leading to their rotation[47,48] towards the graphene planes. Then, strong enough in-plane fields ($B > 0.2$ T) orients the ferromagnetic moments and suppresses the Josephson tunneling between superconducting "grains", leading to the minimum in the resistance and the reentrance to the normal state at lower temperatures, see Fig. 7. The complete suppression of the superconducting transition by the out-of-plane magnetic field of 0.2 T as well as the reappearance of the superconducting transition in (quantized) magnetic fields should be taken as a clear manifestation of orbital effects, absent in the parallel field geometry. Noting also that high enough perpendicular magnetic fields can rotate the ferromagnetic moments in the field direction suppressing the Josephson "intergrain" coupling, both orbital and "spin" effects play a role for this field direction. Evidence for a ferromagnetic response can be obtained from the magnetoresistance for parallel field direction, as was published recently for a similar multigraphene sample.[37]

V. CONCLUSION

We studied the behavior of the resistance of several multigraphene samples as a function of temperature and magnetic field and under the influence of a bias voltage applied normal to the graphene planes. Taking into account relevant literature on granular superconductors as well as the one obtained recently for the internal interfaces in graphite samples, it appears natural to assume that the transition in the resistance that develops at $T \sim 15$ K with negative bias voltage is related to a non-percolative superconducting-like state. The results indicate that a negative voltage increases the carrier density and the Fermi level in certain regions of the samples achieving the necessary minimum density to trigger superconductivity. Shubnikov-de Haas oscillations in the magnetoresistance and above 4 T indicate an increase in average of the carrier density of one order of magnitude relative to the one obtained in bulk graphite samples (without bias voltage). A large enough magnetic field in both directions suppresses the transition. However, we found quantitative and qualitative differences in the behavior of the resistance upon field direction. The overall results also indicate that the carrier density is not homogeneous in the studied multigraphene samples in agreement with previous reports based on EFM and SdH oscillations experiments.

This work is supported by the Deutsche Forschungsgemeinschaft under contract DFG ES 86/16-1 and by the DAAD project under PROBRAL 50724695 and CAPES 339/10. R.R.d.S. and Y.K. acknowledge the support from FAPESP, CNPq, ROBOCON, and INCT NAMITEC. S.D. was supported by the Graduate School of Natural Sciences "BuildMoNa" of the University of Leipzig.

---

[*] esquin@physik.uni-leipzig.de

[1] K. Ueno, S. Nakamura, H. Shimotani, H. T. Yuan, N. Kimura, T. Nojima, H. Aoki, Y. Iwasa, and M. Kawasaki. Electric-field-induced superconductivity in an insulator. Nature Mater., 7:855–858, 2008.

[2] J. T. Ye, S. Inoue, K. Kobayashi, Y. Kasahara, H. T. Yuan, H. Shimotani, and Y. Iwasa. Liquid-gated interface superconductivity on an atomically flat film. Nature Materials, 9:125–128, 2010.

[3] K. Ueno, S. Nakamura, H. Shimotani, H. T. Yuan, N. Kimura, T. Nojima, H. Aoki, Y. Iwasa, and M. Kawasaki. Discovery of superconductivity in ktao$_3$ by electrostatic carrier doping. Nature Nanotechnology, 6:408–412, 2011.

[4] J. Biscaras, N. Bergeal, S. Hurand, C. Grossetêete, A. Rastogi, R. C. Budhani, D. LeBoeuf, C. Proust, and J. Lesueur. Two-dimensional superconductivity induced by high-mobility carrier doping in latio$_3$ /srtio$_3$ heterostructures. arXiv:1112.2633, unpublished.

[5] S. A. Brazovskii and V. M. Yakovenko. Solid State Commun., 132:290, 1988.

[6] Y. Kopelevich and P. Esquinazi. Ferromagnetism and superconductivity in carbon-based systems. J. Low Temp. Phys., 146:629–639, 2007. and refs. therein.

[7] J. González, F. Guinea, and M. A. H. Vozmediano. Electron-electron interactions in graphene sheets. Phys. Rev. B, 63:134421–1–8, 2001.

[8] A. M. Black-Schaffer and S. Doniach. Resonating valence bonds and mean-field d-wave superconductivity in graphite. Phys. Rev. B, 75:134512, 2007.

[9] N. García and P. Esquinazi. Mean field superconductivity approach in two dimensions. J Supercond Nov Magn, 22:439–444, 2009.

[10] Bruno Uchoa and A. H. Castro Neto. Superconducting states of pure and doped graphene. Phys. Rev. Lett., 98:146801, 2007.

[11] N. B. Kopnin and E. B. Sonin. Bcs superconductivity of dirac electrons in graphene layers. Phys. Rev. Lett., 100:246808, 2008.

[12] Sandeep Pathak, Vijay B. Shenoy, and G. Baskaran. Possible high-temperature superconducting state with a $d+id$ pairing symmetry in doped graphene. Phys. Rev. B,

81:085431, 2010.

[13] S. W. Han, J. D. Lee, J. P. Noh, and D. W. Jung. Superconductivity of a calcium-doped graphite CaC_{30}. J. Low Temp. Phys., 160:41–48, 2010.

[14] G. Csányi, P. B. Littlewood, A. H. Nevidomskyy, C. J. Pickard, and B. D. Simons. The role of the interlayer state in the electronic structure of superconducting graphite intercalated compounds. Nature Physics, 1:42–45, 2005.

[15] A. Arndt, D. Spoddig, P. Esquinazi, J. Barzola-Quiquia, S. Dusari, and T. Butz. Electric carrier concentration in graphite: Dependence of electrical resistivity and magnetoresistance on defect concentration. Phys. Rev. B, 80:195402, 2009.

[16] S. Dusari, J. Barzola-Quiquia, P. Esquinazi, and N. García. Ballistic transport at room temperature in micrometer-size graphite flakes. Phys. Rev. B, 83:125402, 2011.

[17] J. Barzola-Quiquia, J.-L. Yao, P. Rödiger, K. Schindler, and P. Esquinazi. Sample size effects on the transport properties of mesoscopic graphite samples. phys. stat. sol. (a), 205:2924–2933, 2008.

[18] N. B. Kopnin, T. T. Heikkilä, and G. E. Volovik. High-temperature surface superconductivity in topological flat-band systems. Phys. Rev. B, 83:220503, 2011.

[19] N. García, P. Esquinazi, J. Barzola-Quiquia, and S. Dusari. Bernal graphite is a narrow gap semiconductor. 2011. arXiv:1106.0437.

[20] M. A. Kuroda, J. Tersoff, and G. J. Martyna. Nonlinear screening in multilayer graphene systems. Phys. Rev. Lett., 106:116804, 2011.

[21] P. Esquinazi, J. Barzola-Quiquia, S. Dusari, and N. García. Length dependence of the resistance in graphite: Influence of ballistic transport. J. Appl. Phys., 111:033709, 2012.

[22] M. Koshino. Interlayer screening effect in graphene multilayers with aba and abc stacking. Phys. Rev. B, 81:125304, 2010.

[23] Y. Zhang, J. P. Small, W. V. Pontius, and P. Kim. Fabrication and electric-field-dependent transport measurements of mesoscopic graphite devices. Appl. Phys. Lett., 86:073104, 2005.

[24] Y. Lu, M. Muñoz, C. S. Steplecaru, Cheng Hao, Ming Bai, N. García, K. Schindler, and P. Esquinazi. Electrostatic force microscopy on oriented graphite surfaces: Coexistence of insulating and conducting behaviors. Phys. Rev. Lett., 97:076805, 2006. See also the comment by S. Sadewasser and Th. Glatzel, Phys. Rev. lett. **98**, 269701 (2007) and the reply by Lu et al., *idem* **98**, 269702 (2007) and also R. Proksch, Appl. Phys. Lett. **89**, 113121 (2006).

[25] H. Kempa, H. C. Semmelhack, P. Esquinazi, and Y. Kopelevich. Absence of metal-insulator transition and coherent interlayer transport in oriented graphite in parallel magnetic fields. Solid State Commun., 125:1–5, 2003.

[26] G. Eiserman R. V. Coleman, M. P. Everson and A. Johnson. Nonlinear magnetotransport and charge-density-wave motion in $nbse_3$ at temperatures from 1.2 to 50 k. Phys. Rev. B, 32:537–540, 1985.

[27] M. P. Everson, G. Eiserman, A. Johnson, and R. V. Coleman. Magnetic- and electric-field-induced transitions at high currents in $nbse_3$ at temperatures from 1.2 to 4.2 k. Phys. Rev. B, 32:541–544, 1985.

[28] S. Parashar, E.E. Ebenso, A.R. Raju, and C.N.R. Rao. Insulatormetal transitions induced by electric and magnetic fields, in thin films of charge-ordered $pr_{1-x}ca_xmno_3$. Solid State Commun., 114:195–299, 2000.

[29] H. M. Jaeger, D. B. Haviland, B. G. Orr, and A. M. Goldman. Onset of superconductivity in ultrathin granular metal films. Phys. Rev. B, 40:182–196, Jul 1989.

[30] C. Christiansen, L. M. Hernandez, and A. M. Goldman. Evidence of collective charge behavior in the insulating state of ultrathin films of superconducting metals. Phys. Rev. Lett., 88:037004, Jan 2002.

[31] Y. Kopelevich, V. Lemanov, S. Moehlecke, and J.H.S. Torres. Landau level quantization and possible superconducting instabilities in highly oriented pyrolitic graphite. Phys. Solid State, 41:1959–1962, 1999.

[32] H. Kempa, Y. Kopelevich, F. Mrowka, A. Setzer, J. H. S. Torres, R. Höhne, and P. Esquinazi. Magnetic field driven superconductor-insulator-type transition in graphite. Solid State Commun., 115:539–542, 2000.

[33] X. Du, S.-W. Tsai, D. L. Maslov, and A. F. Hebard. Metal-insulator-like behavior in semimetallic bismuth and graphite. Phys. Rev. Lett., 94:166601, 2005.

[34] Y. Kopelevich, P. Esquinazi, J.H.S. Torres, and S. Moehlecke. Ferromagnetic- and superconducting-like behavior of graphite. J. Low Temp. Phys., 119:691–702, 2000.

[35] P. Esquinazi, N. García, J. Barzola-Quiquia, P. Rödiger, K. Schindler, J.-L. Yao, and M. Ziese. Indications for intrinsic superconductivity in highly oriented pyrolytic graphite. Phys. Rev. B, 78:134516, 2008.

[36] S. Dusari, J. Barzola-Quiquia, and P. Esquinazi. Superconducting behavior of interfaces in graphite: Transport measurements of micro-constrictions. J Supercond Nov Magn, 24:401–405, 2011.

[37] J. Barzola-Quiquia and P. Esquinazi. Ferromagnetic- and superconducting-like behavior of the electrical resistance of an inhomogeneous graphite flake. J Supercond Nov Magn, 23:451–455, 2010.

[38] Y. Kopelevich, P. Esquinazi, J. Torres, R. da Silva, H. Kempa, F. Mrowka, and R. Ocaña. Studies of High Temperature Superconductors, volume 45, chapter 3, pages 59–106. Nova Science Publishers, Inc., 2003. ISBN 1-59033-697-6.

[39] Y. Shapira and G. Deutscher. Semiconductor-superconductor transition in granular al-ge. Phys. Rev. B, 27:4463–4466, 1983.

[40] J. Barzola-Quiquia, A. Ballestar, S. Dusari, and P. Esquinazi. Experimental Study of the Intrinsic and Extrinsic Transport Properties of Graphite and Multigraphene Samples, chapter 8 *Graphene*. Intech, Open Access Publisher, 2011. ISBN 978-953-307-292-0.

[41] R. Ricardo da Silva, J. H. S. Torres, and Y. Kopelevich. Indication of superconductivity at 35 k in graphite-sulfur composites. Phys. Rev. Lett., 87:147001–1–4, 2001.

[42] H.-P. Yang, H.-H. Wen, Z.-W. Zhao, and S.-L. Li. Possible superconductivity at 37 k in graphite-sulfur composites. Chin. Phys. Lett., 18:1648–1650, 2001.

[43] S. Moehlecke, P. C. Ho, and M. B. Maple. Coexistence of superconductivity and ferromagnetism in the graphite-sulphur system. Phil. Mag. B, 82:1335–1347, 2002.

[44] Israel Felner and Yakov Kopelevich. Magnetization measurement of a possible high-temperature superconducting state in amorphous carbon doped with sulfur. Phys. Rev. B, 79:233409, Jun 2009.

[45] T. D. Moore and D. A. Williams. Andreev reflection at high magnetic fields. Phys. Rev. B, 59:7308, 1999.

[46] S. Moehlecke, Y. Kopelevich, and M. B. Maple. Interaction between superconducting and ferromagnetic order parameters in graphite-sulfur composites. Phys. Rev. B,

69:134519, Apr 2004.

[47] K. Capelle, G. Vignale, and B. L. Györffy. Spin currents and spin dynamics in time-dependent density-functional theory. Phys. Rev. Lett., 87:206403, 2001.

[48] K. Capelle. Exchange-correlation effects in magnetic-field-induced superconductivity. Phys. Rev. B, 65:100515, 2002.